A truly meshless Galerkin method based on a moving least squares quadrature

Marc Duflot*†, Hung Nguyen-Dang

Abstract

A new body integration technique is presented and applied to the evaluation of the stiffness matrix and the body load vector of elastostatic problems obtained by a meshless method. It does not rely on a partition of the integration domain into small cells, but rather on a partition of unity by a set of moving least squares shape functions each defined on a small patch that belongs to a set of overlapping patches covering the domain and so leads to a truly meshless method. We present results demonstrating that this method is specially useful when the nodes are irregularly scattered.

Key-words: meshless method, meshless quadrature.

1 Introduction

Over the last decade, meshless methods for the solution of partial differential equations (PDE) have become increasingly popular. The main idea of these methods is to approximate the unknown field by a linear combination of shape functions built without having recourse to a mesh of the domain. Instead, nodes are scattered in the domain and a certain weight function with a local support is associated with each of these nodes. The shape function associated with a given node is then built considering the weight functions whose support overlaps the one of the weight function of this node; thus, there is actually no need to establish connectivities between the different nodes as in the finite element method. Although the construction of the shape functions is more expensive for meshless methods than for the latter one, they are prime methods for problems with moving boundaries such as crack propagation problems because no remeshing of the domain is necessary.

The coefficients of this linear combination of shape functions are generally obtained by minimizing the residuals of a discrete Galerkin weak form of the PDEs of the problem to solve, so an integration on the domain is needed. In

*FNRS Research Fellow.

†Correspondence to: Marc Duflot, Fracture mechanics department, University of Liège, Chemin des chevreuils 1, 4000 Liège, Belgium. E-mail: m.duflot@ulg.ac.be.

most meshless methods, like in the most popular one, the element-free Galerkin method developed by Belytschko, Lu and Gu [1], this is realized with the help of a background mesh. The purpose of the present paper is to develop a domain integration procedure that does not rely on a partition of the domain into small cells, but rather on a partition of unity [2] by a set of moving least squares (MLS) shape functions, each defined on a small patch which belongs to a set of overlapping patches covering the domain. The application of this procedure to evaluating the stiffness matrix and the body load vector of elastostatic problems obtained by the element-free Galerkin method constitutes a *truly meshless Galerkin method*.

Other truly meshless methods have been proposed. A number of them rely on a nodal integration: Domain integration is approximated by the sum of the products of the integrand at the nodes times a weight representing the fraction of the total area "occupied" by this node. Though this method is quite simple, it suffers from two drawbacks. First, it is unclear how to assign each node a weight. Secondly, the solution presents spatial oscillations that result from under-integration. Beissel and Belytschko [3] on one hand and Nagashima [4] on the other hand add stabilization terms that smooth these oscillations; but these terms may be time-consuming because they require higher-order derivatives of the shape functions. A corrected smooth particle hydrodynamics method by Bonet and Kulasegaram [5] does not need higher-order derivatives but is based on the iterative computation of a stabilization gradient at each node. Chen *et al.* [6] modify the shape functions prior to nodal integration in order to stabilize the solution, but this requires the construction of a Voronoi diagram; so this method does not really qualify as truly meshless.

Atluri and Zhu [7] propose two different truly meshless methods. Both use a non-Galerkin weak form in order to avoid the need for a background mesh. The first is the local boundary integral equation method that only needs integration on paths surrounding the nodes if the PDEs are linear and without body load. The second is the meshless local Petrov-Galerkin method that needs integrations on subdomains surrounding the nodes. The main drawback of both of these methods is that the resulting stiffness matrix is not symmetric, which is not the case in the present method.

Finally, the method of finite spheres of De and Bathe [8] consists in integrating on the intersections of each pair of overlapping spherical supports separately. This requires a greater number of points than the methods previously mentioned and than our new method, since the integrations are performed on a large number of lens-shaped domains.

2 Moving least squares approximation

Construction of the MLS shape functions Consider a set of N nodes scattered in a domain Ω and let $\mathbf{x}_i$ be the coordinates of the node i. The moving least squares approximation (MLSA) $\mathbf{u}^h(\mathbf{x})$ of a (multi-dimensional)

field $\mathbf{u}(\mathbf{x})$ in Ω is (see [1] for details):

$$\mathbf{u}^h(\mathbf{x}) = \sum_{i=1}^{N} \phi_i(\mathbf{x})\,\mathbf{u}_i \tag{1}$$

where $\mathbf{u}_i$ is the value of the field $\mathbf{u}$ at $\mathbf{x}_i$ and ϕ_i is the shape function of the node i, given by

$$\phi_i(\mathbf{x}) = \mathbf{c}^{\mathrm{T}}(\mathbf{x})\,\mathbf{p}(\mathbf{x}_i)\,w_i(\mathbf{x}) \tag{2}$$

where $\mathbf{p}(\mathbf{x})$ is a set of basis functions, $w_i(\mathbf{x})$ is a weight function associated with the node i and

$$\mathbf{c}(\mathbf{x}) = \mathbf{A}^{-1}(\mathbf{x})\,\mathbf{p}(\mathbf{x}) \tag{3}$$

with

$$\mathbf{A}(\mathbf{x}) = \sum_{i=1}^{N} w_i(\mathbf{x})\,\mathbf{p}(\mathbf{x}_i)\,\mathbf{p}^{\mathrm{T}}(\mathbf{x}_i) \tag{4}$$

Choice of the basis functions The set of the basis functions is chosen as the set of all the monomials up to a given order. So, in 2D problems, the constant basis is just $\mathbf{p}^{\mathrm{T}}(\mathbf{x}) = [1]$, the linear basis is $\mathbf{p}^{\mathrm{T}}(\mathbf{x}) = [1\; x\; y]$ and the quadratic basis is $\mathbf{p}^{\mathrm{T}}(\mathbf{x}) = \left[1\; x\; y\; x^2\; xy\; y^2\right]$. The MLSA is consistent i.e. the shape functions exactly reproduce all the functions within the span of the basis $\mathbf{p}(\mathbf{x})$. Since the constant function is always included in the set, this implies that

$$\sum_{i=1}^{n} \phi_i(\mathbf{x}) = 1 \qquad \forall \mathbf{x} \in \Omega \tag{5}$$

The particular case of the MLSA with a constant basis is known as the Shepard approximation [9] and leads to a simpler form for the shape functions than other choices because the matrix $\mathbf{A}(\mathbf{x})$ is reduced to a 1×1 size. The cost of the computation of the shape functions is then lower than for the other choices because they are simply given by

$$\phi_i^{\text{Shepard}}(\mathbf{x}) = \frac{w_i(\mathbf{x})}{\sum_{j=1}^{n^{\mathbf{x}}} w_j(\mathbf{x})} \tag{6}$$

In the numerical examples of section 5, we use a linear set of basis functions in the construction of the MLSA of the displacement field, but the Shepard functions will also be useful in section 4.

Choice of the weight functions We make the choice that the function $w_i(\mathbf{x})$ is only strictly positive in a sub-domain Ω_i containing $\mathbf{x}_i$ but is zero outside this Ω_i, which is called the support of the function $w_i(\mathbf{x})$ or the domain of influence of the node $\mathbf{x}_i$. This choice is made in order to give the approximation a local character and to restrict the sums in equations (1) and (4) to a few terms. Moreover, we also decide that $w_i(\mathbf{x})$ decreases with the distance between $\mathbf{x}_i$ and $\mathbf{x}$ so that the nearer a node is to a point, the greater it influences this point.

Several weight functions can be used. A review of some of the possibilities can be found in [10]. In this work, we use the quartic spline expressed as follows:

$$w_4(s) = \begin{cases} 1 - 6s^2 + 8s^3 - 3s^4 & \text{if } |s| \leq 1 \\ 0 & \text{if } |s| > 1 \end{cases} \tag{7}$$

In the construction of the MLSA of the displacement field, we use circular supports: $w_i(\mathbf{x}) = w_4(\frac{\|\mathbf{x}-\mathbf{x}_i\|}{r_i})$ where r_i is the radius of the domain of influence of the node i. But, in section 4, we also use rectangular supports: $w_i(\mathbf{x}) = w_4(\frac{x-x_i}{\Delta x_i}).w_4(\frac{y-y_i}{\Delta y_i})$ (in two-dimensional problems) where Δx_i and Δy_i are half the sides of the domain of influence of the node i. The weight function with a circular support is called isotropic weight function, and the one with rectangular support, tensor-product weight function.

3 Discrete equations of the Galerkin weak form

In this section, we recall the discrete Galerkin modified weak form of the equilibrium equations of linear elasticity. The modification of the weak form is necessary to enforce the essential boundary conditions since the Kronecker delta property is not verified. We refer to [11] for details.

The displacement field in a solid that occupies a domain Ω bounded by Γ subject to the body force $\mathbf{b}$ in Ω, to the surface tractions $\overline{\mathbf{t}}$ on Γ_t and with prescribed displacements $\overline{\mathbf{u}}$ on Γ_u (with $\Gamma_t \bigcap \Gamma_u = \emptyset$ and $\Gamma_t \bigcup \Gamma_u = \Gamma$) is approximated by

$$\mathbf{u}^h(\mathbf{x}) = \sum_{i=1}^{n} \phi_i(\mathbf{x})\, \mathbf{u}_i \tag{8}$$

where the $\phi_i(\mathbf{x})$ are the MLS shape functions (2) and the $\mathbf{u}_i$ are arranged in a vector $\mathbf{q}$ that is determined by

$$\mathbf{K}\mathbf{q} = \mathbf{g} \tag{9}$$

with $\mathbf{K}$ consisting in submatrices $\mathbf{K}_{ij}$ of size $n_{\text{dim}} \times n_{\text{dim}}$ and $\mathbf{g}$ consisting in subvectors $\mathbf{g}_i$ of size n_{dim} given by

$$\mathbf{K}_{ij} = \int_\Omega \mathbf{B}_i^{\mathrm{T}} \mathbf{D} \mathbf{B}_j \,\mathrm{d}\Omega - \int_{\Gamma_u} \left(\phi_i \mathbf{S} \mathbf{N} \mathbf{D} \mathbf{B}_j + \mathbf{B}_i^{\mathrm{T}} \mathbf{D}^{\mathrm{T}} \mathbf{N}^{\mathrm{T}} \mathbf{S} \phi_j \right) \mathrm{d}\Gamma \tag{10}$$

$$\mathbf{g}_i = \int_{\Gamma_t} \phi_i \overline{\mathbf{t}} \,\mathrm{d}\Gamma + \int_\Omega \phi_i \mathbf{b} \,\mathrm{d}\Omega - \int_{\Gamma_u} \mathbf{B}_i^{\mathrm{T}} \mathbf{D}^{\mathrm{T}} \mathbf{N}^{\mathrm{T}} \mathbf{S} \overline{\mathbf{u}} \,\mathrm{d}\Gamma \tag{11}$$

In the two-dimensional problems considered in section 5, we have

$$\mathbf{B}_i = \begin{pmatrix} \phi_{i,x} & 0 \\ 0 & \phi_{i,y} \\ \phi_{i,y} & \phi_{i,x} \end{pmatrix} \tag{12}$$

$$\mathbf{N} = \begin{pmatrix} n_x & 0 & n_y \\ 0 & n_y & n_x \end{pmatrix} \tag{13}$$

$$\mathbf{S} = \begin{pmatrix} s_x & 0 \\ 0 & s_y \end{pmatrix} \tag{14}$$

where $\mathbf{n}$ is the unit outward normal to the boundary and where $s_k = 1$ if u_k is prescribed on Γ_u and $s_k = 0$ either. And finally, for plane stress problems,

$$\mathbf{D} = \frac{E}{1-\nu^2} \begin{pmatrix} 1 & \nu & 0 \\ \nu & 1 & 0 \\ 0 & 0 & \frac{1-\nu}{2} \end{pmatrix} \tag{15}$$

where E and ν are Young modulus and Poisson ratio, respectively.

4 Numerical integration of the weak form

In this paper, we are concerned with the body contribution of (10) and (11):

$$\mathbf{K}_{ij}^{\text{body}} = \int_\Omega \mathbf{B}_i^{\mathrm{T}} \mathbf{D} \mathbf{B}_j \, \mathrm{d}\Omega \tag{16}$$

$$\mathbf{g}_i^{\text{body}} = \int_\Omega \phi_i \mathbf{b} \, \mathrm{d}\Omega \tag{17}$$

but first we shall discuss an integration technique applicable to any function $f(\mathbf{x})$ on Ω.

To that end, we consider a set of l functions $\psi_k(\mathbf{x})$ that verifies the following properties:

1. a patch Ω_k is associated with each ψ_k and is such that $\psi_k(\mathbf{x}) = 0$ if $\mathbf{x} \notin \Omega_k$,
2. the patches cover the domain: $\Omega \subset \bigcup_{k=1}^{l} \Omega_k$,
3. the set of functions partitions the unity: $\sum_{k=1}^{l} \psi_k(\mathbf{x}) = 1 \ \forall \mathbf{x} \in \Omega$.

We note that the Ω_k may overlap each other or not. Thanks to this set of functions, we have:

$$\int_\Omega f(\mathbf{x}) \, \mathrm{d}\Omega = \sum_{k=1}^{l} \int_{\Omega \cap \Omega_k} \psi_k(\mathbf{x}) \, f(\mathbf{x}) \, \mathrm{d}\Omega \tag{18}$$

and we obtain an estimation of the integral of $f(\mathbf{x})$ on Ω by performing a Gaussian quadrature of the functions $\psi_k(\mathbf{x}) \, f(\mathbf{x})$ on the subdomains $\Omega \cap \Omega_k$ $(k = 1, 2, \ldots, l)$ and by adding these contributions.

From a practical point of view, it is recommended to choose a simple geometry for the Ω_k, so that the quadrature is easy to perform on these patches (and on their intersection with Ω for those that are cut by the boundary).

The traditional integration technique can be seen as a particular case of this technique: the Ω_k are the cells of a partition of Ω we must make, and $\psi_k(\mathbf{x}) = 1$ if $\mathbf{x} \in \Omega_k$ and 0 otherwise. The three properties are actually verified and the

integral of $f(\mathbf{x})$ is simply estimated by the sum of the quadratures of $f(\mathbf{x})$ on the different cells of the partition of Ω.

Another possibility is to take a set of MLS shape functions. This procedure is called the moving least squares quadrature (MLSQ). The first property is verified since a shape function is zero outside its support. If this set of MLS shape functions is well defined, there are at least m non-zero ψ_k at each point, where m is the number of functions in the basis; so, the second property is verified. The last property is also verified, by the consistency property of the MLS, since the constant function is always included in the set of basis functions $\mathbf{p}(\mathbf{x})$. The computationally most efficient choice is to take the Shepard shape functions (6). For the sake of simplicity, we also choose tensor-product weight functions in order to be able to integrate on rectangles (resp. parallelepiped in 3D), which is easier than integrating on circles (resp. spheres). The easiest way to deal with curved boundaries is to integrate on the rectangular patches Ω_k and to give a weight equal to zero to the quadrature points outside the domain Ω. This comes down to using the following equation

$$\int_{\Omega\cap\Omega_k} \psi_k(\mathbf{x})\, f(\mathbf{x})\, \mathrm{d}\Omega = \int_{\Omega_k} \psi_k(\mathbf{x})\, f(\mathbf{x})\, \delta_\Omega(\mathbf{x})\, \mathrm{d}\Omega \tag{19}$$

where

$$\delta_\Omega(\mathbf{x}) = \begin{cases} 1 \text{ if } \mathbf{x} \in \Omega \\ 0 \text{ if } \mathbf{x} \notin \Omega \end{cases} \tag{20}$$

It is wise, however, to use a greater number of points in those patches that are cut by the boundary than in the other patches.

Now that the meshless integration procedure is introduced, let's come back to the particular case of (16) and (17). To avoid long repetitions, we denote in the following Φ the set of the shape functions $\phi_i(\mathbf{x})$ used for the MLSA of the unknown field, and Ψ the set of the shape functions $\psi_k(\mathbf{x})$ used by the MLSQ.

The ϕ_i and their derivatives appear in integrals (16) and (17). So, we take into account the scattering of the nodes and the size of the supports of set Φ to build set Ψ. More precisely, we decide that the nodes of the two sets coincide and that the size of a rectangular support of Ψ depends on the size of the associated support of Φ: the supports of Ψ must be big enough to cover Ω, but we choose them small enough so that a support of Ψ is included in the associated support of Φ. The additional cost of this new integration procedure allowing us to obtain a truly meshless method is low with respect to the total cost of a meshless method because:

- Ψ uses Shepard approximation (6) which is cheaper than other approximations (2), such as the one used by Φ.
- The derivatives of the shape functions of Ψ are not needed unlike those of Φ,
- At a given point, the computation of the shape functions of Ψ is done after that of Φ. So, it is easy to determine which nodes influence this

point in Ψ. It is actually only necessary to search them among the ones that influence the point in Φ since each support of Ψ is included in the corresponding support of Φ.

5 Numerical results

We demonstrate the simplicity and power of our method on the near-tip crack problem. We need the asymptotic displacement field for mode I crack that is given in e.g. [12] as

$$\mathbf{u} = \begin{pmatrix} \frac{K_I}{2\mu}\sqrt{\frac{r}{2\pi}}\cos\left(\frac{\theta}{2}\right)\left[\kappa - 1 + 2\sin^2\left(\frac{\theta}{2}\right)\right] \\ \frac{K_I}{2\mu}\sqrt{\frac{r}{2\pi}}\sin\left(\frac{\theta}{2}\right)\left[\kappa + 1 - 2\cos^2\left(\frac{\theta}{2}\right)\right] \end{pmatrix} \tag{21}$$

where μ is the shear modulus defined as $\frac{E}{2(1+\nu)}$, κ is the Kolosov constant defined as $\frac{3-\nu}{1+\nu}$ for plane stress, r is the distance from the crack tip and θ is the angle measured from a line ahead of the crack (see Fig. 1).

In our numerical tests, twofold symmetry is used. The domain is a square with side w. The crack lies in a part of length a of the lower side and is free of load. The displacement perpendicularly to the crack is zero in the rest of this side. The exact displacement (21) is prescribed on the three other sides. We use the following numerical values: $w = 1$, $a = 0.3$, $E = 1$, $\nu = 0.25$ and $K_I = 1$.

We use two irregular sets of nodes. The first one is moderately refined around the crack tip (178 nodes, Fig. 2a) and the second is highly refined (676 nodes, Fig. 2b). The radius r_i of the supports of Φ is $1,4\,h_i$ and the half-side of the squares that are the supports of Ψ is $0,8\,h_i$ where h_i is the distance from the node i to its first neighbor. We use 12×12 quadrature points in each subdomain. We compare the MLSQ with a traditional integration on a regular grid with 8×8 points in each cell; the number of cells is such that the total number of quadrature points is nearly the same as with the integration on Ψ (that means 20×20 cells for the first set and 40×40 for the second).

We compare the different methods by examining the computed mode I stress intensity factor K_I. It is evaluated by using the path independent J integral converted into a domain integral [13]. The computed K_I for a range of the size of this domain for the two sets of nodes with each of the two integration procedures is plotted in Fig. 3.

We note that the results are better if we use a big domain for the computation of J. For a given integration procedure, the highly refined set gives better results than the moderately refined set as expected. More important is the fact that, for a given set, the MLSQ gives better results than the integration on regular grid whereas both techniques possess (nearly) the same number of quadrature points. This is due to the fact that, when the integration is performed on Ψ, the points are "better located": a large number of them are near the crack tip where the number of nodes of Φ is high and thus where the integrands vary a lot. We insist on the fact that this concentration of the points is automatic with the new technique. Of course, we can imagine building an irregular grid

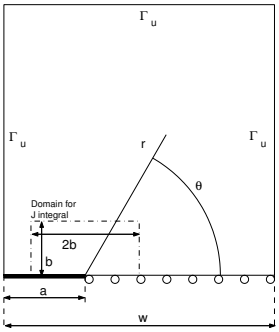

Figure 1: Near-tip crack problem

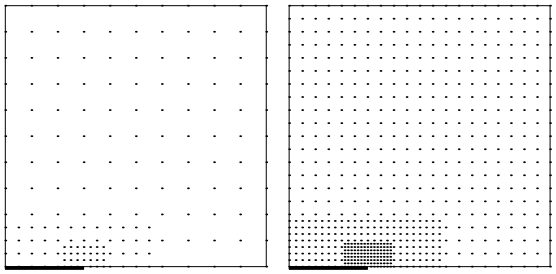

(a) the moderately refined set (178 nodes)

(b) the highly refined set (676 nodes)

Figure 2: The two sets of nodes used to solve the near-tip crack problem

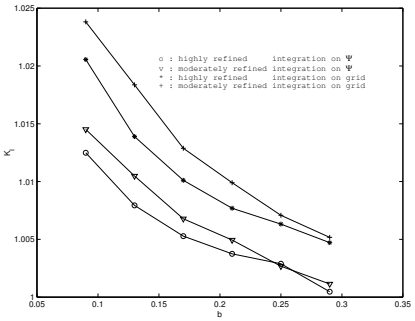

Figure 3: Mode I stress intensity factor for the near-tip crack problem

with smaller cells near the crack tip and performing the traditional integration technique on each cell, but this is a mesh of the domain — and this is precisely what we want to avoid.

6 Conclusions

We have presented a meshless method that does not rely on any background mesh. The method is applicable to any type of problem with any number of dimensions. Here, we have presented a numerical test for a 2D elasticity problem. The test has clearly demonstrated the efficiency of the method.

We find this new method both simple and smart because the integration scheme is related to the set of nodes used for the approximation. So, the quadrature points concentrate automatically where the node density is high. We may thus expect that this method will be particularly useful in adaptive computations, since an increase in the number of nodes in a given area will involve an increase in the number of quadrature points in this area. We also expect that our method will be found specially simple for 3D problems with complicated shapes.

Acknowledgements

The support of the Belgian National Fund for Scientific Research (F.N.R.S.) for Marc Duflot is gratefully acknowledged.

References

[1] Belytschko T, Lu YY, Gu L. Element-free Galerkin methods. *International Journal for Numerical Methods in Engineering* 1994; **37**:229–256.

[2] Melenk JM, Babuska I. The partition of unity finite element method: Basic theory and applications. *Computer Methods in Applied Mechanics and Engineering* 1996; **139**:289–314.

[3] Beissel S, Belytschko T. Nodal integration of the element-free Galerkin method. *Computer Methods in Applied Mechanics and Engineering* 1996; **139**:49–74.

[4] Nagashima T. Node-by-node meshless approach and its applications to structural analyses. *International Journal for Numerical Methods in Engineering* 1999; **46**:341–385.

[5] Bonet J, Kulasegaram S. Correction and stabilization of smooth particle hydrodynamics methods with applications in metal forming simulations. *International Journal for Numerical Methods in Engineering* 2000; **47**:1189–1214.

[6] Chen JS, Wu CT, Yoon S, You Y. A stabilized conforming nodal integration for Galerkin mesh-free methods. *International Journal for Numerical Methods in Engineering* 2001; **50**:435–466.

[7] Atluri SN, Zhu T. New concepts in meshless methods. *International Journal for Numerical Methods in Engineering* 2000; **47**:537–556.

[8] De S, Bathe KJ. Displacement/pressure mixed interpolation in the method of finite spheres. *International Journal for Numerical Methods in Engineering* 2001; **51**:275–292.

[9] Shepard D. A two-dimensional function for irregularly spaced points. In *23rd ACM National Conference*, 1968; 517–524.

[10] Belytschko T, Krongauz Y, Organ D, Fleming M, Krysl P. Meshless methods: An overview and recent developments. *Computer Methods in Applied Mechanics and Engineering* 1996; **139**:3–47.

[11] Lu YY, Belytschko T, Gu L. A new implementation of the element-free Galerkin method. *Computer Methods in Applied Mechanics and Engineering* 1994; **113**:397–414.

[12] Anderson TL. *Fracture Mechanics: Fundamentals and Applications*. CRC Press, 1991.

[13] Moran B, Shih CF. Crack tip and associated domain integrals from momentum and energy balance. *Engineering Fracture Mechanics* 1987; **27**(6):615–641.